

Restriction Spectrum Imaging of Glioblastoma Multiforme: Comparison vs. ADC.

Nathan White¹, Joshua Kuperman¹, Carrie McDonald², Nikdokht Farid¹, Santosh Kasari³, Ajit Shankaranarayanan⁴, and Anders Dale^{1,5}

¹Department of Radiology, University of California, San Diego, La Jolla, CA, United States, ²Department of Psychiatry, University of California, San Diego, La Jolla, CA, United States, ³Department of Neuro-Oncology, University of California, San Diego, La Jolla, CA, United States, ⁴GE Healthcare, Inc., ⁵Department of Neuroscience, University of California, San Diego

Introduction

Diffusion-weighted MRI (DW-MRI) offers a unique perspective on tumor pathology by probing the microscopic diffusion properties of neoplastic tissue at the cellular and subcellular level [1]. Measurements of the bulk apparent diffusion coefficient (ADC) of malignant neoplasms are often reported *reduced* compared with healthy tissue, consistent with an increase fraction of slow restricted diffusion associated with high cellular microenvironments [2]. However, the ADC is unspecific, and is sensitive to numerous other secondary factors including tumor and treatment related cytotoxic and vasogenic edema and necrosis. Moreover, many of these factors are thought to cause a concomitant *increase* in ADC by reducing the tortuosity of the extracellular matrix thereby increasing the fraction of fast hindered diffusion [2]. Multi-b-value DW-MRI scans over an extended range ($b > 3000 \text{ s/mm}^2$) may allow hindered and restricted water compartments to be distinguished, thereby providing more sensitive and specific biomarkers of tumor pathology. We have recently introduced a method for multi-b-value / multi-diffusion time DW-MRI called "Restriction Spectrum Imaging" (RSI), which models a spectrum of hindered and restricted compartments at different scales and geometries [3]. Here we demonstrate an application of RSI for improved detection / identification of glioblastoma multiforme (GBM) from surrounding healthy and edematous tissue compared with the ADC.

Materials and Methods

Four patients with biopsy confirmed GBM were included in this preliminary study. Ethics board approval and informed consent was obtained. MR imaging was performed on a 3.0T GE Signa Excite scanner equipped with a 12-channel head coil. 3D T2-weighted FLAIR images were acquired (TE/TR = 126/6000ms; TI = 1863ms; FOV = 24cm; $0.93 \times 0.93 \times 1.2 \text{ mm}$), followed by 3D (post-Gad) Sagittal T1-weighted IR-SPGR (TE/TR = 2.8/6.5ms; TI = 450ms; FA = 8° ; FOV = 24cm; $0.93 \times 0.93 \times 1.2 \text{ mm}$) and single-shot spin-echo diffusion-weighted echo-planar imaging (TE/TR = 96ms/17s; FOV = 24cm, matrix = $128 \times 128 \times 48$). Diffusion data were acquired with $b = 0, 500, 1500$, and 4000 s/mm^2 , with 0, 6, 6, and 15 unique gradient directions for each b-value, respectively (28 total, total time ~8min). Diffusion data were corrected offline for spatial distortions due to susceptibility [4] and eddy currents and registered to the 3D anatomical scans. ADC maps were calculated from a tensor fit using the full dataset: $b = 0, 500, 1500$, and 4000 s/mm^2 .

RSI Analysis: With constant diffusion time protocols, the RSI model reduces to a spectrum of ADC's at each voxel of the form [3]: $S = S_0 \exp[-b(\sum_i \text{ADC}_i)]$; $\text{ADC}_i = (\text{ADC}_{||} - \text{ADC}_{\perp,i}) \cos^2 \alpha + \text{ADC}_{\perp,i}$, where $\text{ADC}_{||}$ and ADC_{\perp} are the apparent parallel and perpendicular diffusivities of a cylindrical tissue element, α is the angle between the cylinder (long) axis and the diffusion gradient direction, and S_0 is the signal measured at $b = 0$. To define the spectrum, we set $\text{ADC}_{||} = 1 \times 10^{-3} \text{ mm}^2 \text{ s}^{-1}$ and vary ADC_{\perp} from $0 \text{ mm}^2 \text{ s}^{-1}$ to $\text{ADC}_{||}$ in six equally spaced steps (Fig. 1a, Scales 1-6). Two additional isotropic terms were included, one modeling restricted diffusion ($\text{ADC}_{||} = \text{ADC}_{\perp} = 0 \text{ mm}^2 \text{ s}^{-1}$, Fig 1a, Scale 0) and one "free" water ($\text{ADC}_{||} = \text{ADC}_{\perp} = 3 \times 10^{-3} \text{ mm}^2 \text{ s}^{-1}$, Fig 1a, Scale 7). To account for the unknown orientation of the cylindrical components (Scales 1-6, where $\text{ADC}_{\perp} < \text{ADC}_{||}$), we used a spherical harmonic (SH) parameterization for their orientation distribution [3]. Parameter maps were then fit to the unnormalized signal S , which included the (T2-weighted) ADC volume fractions (Fig 1b) and the SH coefficients (not shown), using least-squares estimation with Tikhonov regularization [3]. A constrained minimum variance beamformer (CMVB) was used to combine the parameter maps into a single image (herein termed the "RSI cellularity index", or RSI-CI) with optimal sensitivity to isotropic restricted diffusion (Scale 0).

Receiver Operating Characteristics (ROC): ROC curves were used to quantify the increase in tumor conspicuity in the RSI-CI maps vs ADC. Regions-of-interest (ROIs) were manually drawn for tumor, peritumoral edema, and non-tumoral normal appearing white matter (NAWM) using co-registered T1-post, FLAIR, and ADC maps in Amira® (Visage Imaging, Inc). The mean and standard deviation (std) (across all subjects) RSI-CI and ADC were calculated for each ROI. ROC curves were generated by plotting the cumulative distribution of voxel intensity histograms across all patients for tumor (sensitivity) vs. NAWM (1-specificity), and the area under the curve (AUC) was calculated.

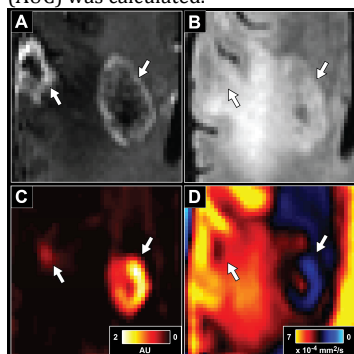


Fig 2. Comparison of RSI-CI vs. ADC in the same patient as Fig 1. (A) T1-post Gd (B) T2-FLAIR (C) RSI-CI (D) ADC. Arrows indicate areas of biopsy confirmed tumor. Note the high sensitivity of ADC to edema (FLAIR hyperintensity). Also note the lateral (left) tumor site that is easily identified by RSI-CI but not ADC.

Results and Discussion

Substantial qualitative improvements in tumor conspicuity and delineation of tumor borders were observed in the RSI-CI maps vs. ADC for all patients (Fig 2, example). As expected, quantitative analysis confirmed the ADC had greater relative sensitivity (ratio of mean signal) to edema vs. tumor (Fig 3B), while RSI-CI demonstrated greater relative sensitivity to tumor vs. edema (Fig 3A). Furthermore, ROC analysis indicated greater tumor detection (classification) accuracy with RSI-CI vs. ADC (AUC = 0.98 vs. 0.82) (Fig 3C). While the ADC continues to be an important clinical biomarker of tumor cellularity, our results here suggest RSI may offer even greater sensitivity and specificity to tumor pathology vs. ADC, especially in the presence of edema. In light of this, RSI may offer more accurate in vivo quantification of tumor cellularity and early detection of tumor infiltration in peritumoral edema (see Fig 2CD) as well as provide a more sensitive and specific biomarker of tumor response to treatment.

References

- [1] Le Bihan D, NMR Biomed. 1995.
- [2] Chenevert TL, NeuroImag Clin N Am, 2006.
- [3] White NS, HBM In press.
- [4] Holland D, NeuroImage. 2010.

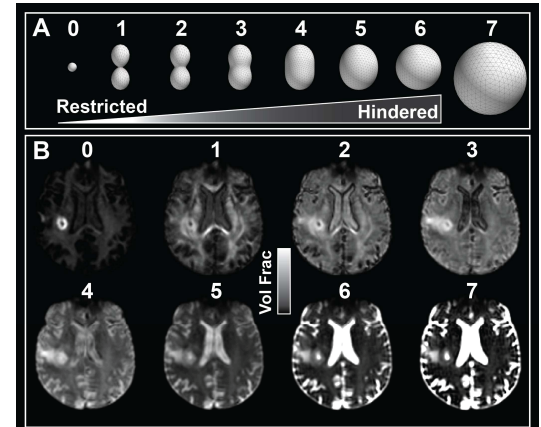


Fig 1. RSI analysis for a single GBM patient. (A) RSI ADC spectrum model. (B) Volume fraction maps for each scale in A. Note the increased volume fraction of isotropic restricted diffusion (Scale 0) in tumor. The RSI-CI map (Fig 2C) was generated from the full spectrum (Scales 0-7) using the CMVB, which enhances signal from Scale 0 and suppresses signal from Scales 1-7 (i.e. suppresses signal from NAWM, edema, CSF, and grey matter).

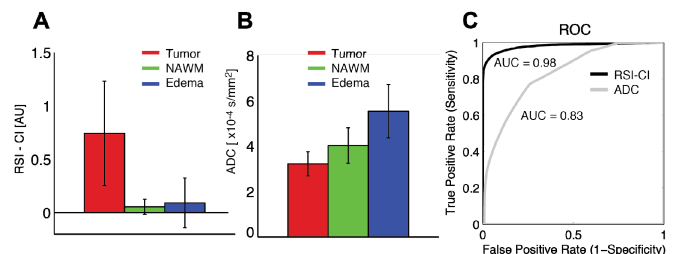


Fig 3. Mean (\pm std) signal (across all subjects) in each ROI for (A) RSI-CI, and (B) ADC. (C) ROC curves for RSI-CI and ADC.